Nat Immunol. Author manuscript; available in PMC 2011 October 01.

Published in final edited form as:
Nat Immunol. 2011 April ; 12(4): 352–361. doi:10.1038/ni.2008.

Phosphoproteomic analysis reveals an intrinsic pathway for histone deacetylase 7 regulation that controls cytotoxic T lymphocyte function

Maria N. Navarro[1], **Jurgen Goebel**[1], **Carmen Feijoo-Carnero**[1], **Nick Morrice**[2], and **Doreen A. Cantrell**[1]

[1]The College of Life Sciences, Division of Immunology and Cell Biology, The University of Dundee, Dundee, Scotland, U.K

[2]The Beatson Institute for Cancer Research, Glasgow, Scotland, U.K

Abstract

The present study reports an unbiased analysis of cytotoxic T cell serine-threonine phosphoproteome using high resolution mass spectrometry. Approximately 2,000 phosphorylations were identified in CTLs of which approximately 450 were controlled by TCR signaling. A significantly overrepresented group of molecules identified were transcription activators, co-repressors and chromatin regulators. A focus on chromatin regulators revealed that CTLs have high expression of histone deacetylase HDAC7 but continually phosphorylate and export this transcriptional repressor from the nucleus. HDAC7 dephosphorylation results in its nuclear accumulation and suppressed expression of genes encoding key cytokines, cytokine receptors and adhesion molecules that determine CTL function. The screening of CTL phosphoproteome thus reveals intrinsic pathways of serine-threonine phosphorylation that target chromatin regulators and determine the CTL functional program.

INTRODUCTION

Recent studies have shown that a network of signal transduction pathways controlled by serine-threonine kinases such as mTOR (mammalian target of rapamycin), members of the AMPK (AMP-activated protein kinase) family and Akt (protein kinase B, PKB) program cytotoxic T lymphocyte (CTL) fate1-8. However, much of what we know about serine kinases in CTLs is based on experiments that confirm or refute the existence of evolutionarily conserved pathways of serine-threonine phosphorylation. For example, Akt mediated phosphorylation of the transcription factors Foxo1 and Foxo3a results in their nuclear exclusion and termination of Foxo-mediated gene transcription. This pathway of Foxo regulation is conserved in CTLs and plays a key role to determine the repertoire of chemokine and adhesion receptors expressed by these cells5,9.

Corresponding author: Doreen Cantrell, Division of Immunology and Cell Biology, University of Dundee, Dundee, DD1 5EH, Scotland, UK. Tel: +44 (0)1382 385047, Fax: +44 (0)1382 385783, d.a.cantrell@dundee.ac.uk.

AUTHOR CONTRIBUTIONS

M.N, J.G and C.FC performed the experiments and analyses the results. N.M supervised SILAC methodology and bioinformatic analysis. M.N and D.C. designed the experiments, analyzed the results and wrote the paper.

DATABASE ACCESION NUMBER

The microarray data discussed in this publication have been deposited in NCBI's Gene Expression Omnibus52 and are accessible through GEO Series accession number GSE27092 (http://www.ncbi.nlm.nih.gov/geo/query/acc.cgi?acc=GSE27092).

Europe PMC Funders Author Manuscripts

A strategy that focuses on conserved serine kinases and their substrates in CTLs is valuable but limited in its potential to uncover novel protein phosphorylations in these important cells. What is needed is an unbiased analysis of the full spectrum of protein phosphorylations in CTLs. In particular defining the intrinsic basal network protein phosphorylations in CTLs should reveal the signaling pathways that maintain the essential epigenetic, transcriptional and metabolic programs that are permissive for CTL function. One way to achieve a global analysis of the cell phosphoproteome is to use mass spectrometry. In particular, Stable Isotope Labeling by Amino acids in cell Culture (SILAC) in combination with phosphopeptide enrichment protocols and high resolution mass spectrometry (MS) provide powerful technologies to probe the cellular phosphoproteome10. The potential value of SILAC protocols is demonstrated by studies of T cell antigen receptor signaling in the T leukemic cell line Jurkat11-13. The SILAC approach involves the incorporation of amino acids with substituted stable isotopic nuclei (in this case deuterium ^{2}H, ^{13}C, ^{15}N) into cells. This strategy allows multiplexing of different conditions and bypasses many of the errors in reproducibility caused by the complex protocols used to purify phosphorylated peptides prior to mass spectrometry. Accordingly the object of the present report was to use SILAC in combination with phosphoprotein enrichment protocols to explore the cytotoxic T cell phosphoproteome. The current experiments identified more than approximately 2,000 phosphorylated peptides in CTLs representative of more than 900 proteins either singly or multiply phosphorylated. Triggering of the TCR with cognate peptide-major histocompatibility (MHC) complexes modulated phosphorylation of approximately 20% of the serine-threonine phosphoproteome of CTLs. The complex network of basal protein phosphorylation in CTLs prior to TCR engagement was striking and afforded insights about links between serine-threonine kinases and chromatin regulators that control the genes encoding important cytokines and cytokine receptors in CTLs. Collectively the experiments reveal the power of unbiased phospho-proteomic analysis to unravel the molecular mechanisms that control CTL fate.

RESULTS

Analysis of the basal and TCR regulated phosphoproteome in CTLs

SILAC labeling requires that cells undergo multiple cell doublings *in vitro*. Accordingly for SILAC experiments with CTLs we used a well-characterized *in vitro* model of CTL differentiation based on the use of T cells from P14 TCR transgenic mice4,14,15. TCR triggered P14 T cells cultured in interleukin 2 (IL-2) produce a homogenous population of effector CTLs14,15. Moreover, this model reproduces the *in vivo* situation where sustained IL-2 signaling promotes the production of terminally differentiated effector cytotoxic T cells16-18. For quantitative analysis of basal and TCR regulated phosphorylations of CTLs, these cells were differentially labeled with one of two different isotope combination of lysine (K) and arginine (R), R0K0 and R10K8 (see schematic workflow in Supplementary Fig. 1). CTLs were then either left unstimulated or triggered via their TCR with cognate peptide. Tryptic peptides from total cellular extracts were then resolved by hydrophilic liquid interaction chromatography (HILIC) followed by phosphopeptide enrichment with immobilized metal ion affinity chromatography (IMAC). Peptides were subsequently separated by high performance liquid chromatography (HPLC) that was coupled in line with a Linear Trap Quadrupole (LTQ)-Orbitrap XL for mass spectrometry (MS) data collection. All raw mass spectrometry data were processed using the MaxQuant software which automatically performed peptide to protein assignment, SILAC-based quantification of peptides and phosphorylation events as well as phosphorylation site localization in identified phosphopeptides.

The focus of the present study was serine and threonine phosphorylations. We identified 2,081 distinct serine-threonine phosphopeptides in CTLs derived from 955 proteins (Fig. 1a,

full list in Supplementary Table 1). 22% of all quantified phosphorylation sites were regulated following TCR engagement. Triggering of the TCR with peptide-MHC complexes thus led to changes in 450 phosphorylation sites of which 391 were up regulated and 59 downregulated (Supplementary Table 1). Importantly, these experiments captured previously described TCR-regulated serine or threonine phosphorylations. For example, TCR triggering induced dephosphorylation of the transcription factor NFAT (Nuclear Factor of Activated T cells)19 and the actin remodeling protein Cofilin20 (Table 1). TCR triggering also increased phosphorylation of the MAP kinases Erk1/2 and the microtubule stabilizing protein Stathmin on residues S25 and S16, which are known to be substrate sites for Erk1/2 and the TCR-regulated calcium-calmodulin dependent kinase IV21. Moreover, Ingenuity Pathway Analysis (Ingenuity® Systems, http://www.ingenuity.com) independently concluded that the identified TCR-regulated phosphoproteins were components of TCR signal transduction pathways (Supplementary Fig. 2) and revealed that a significantly overrepresented molecular function in all identified phosphoproteins was to control gene transcription (Fig. 1b).

To determine the biological reproducibility of the results in Fig. 1 we repeated the experiments four times including amino acid labeling switch. Collective analysis of pooled data from multiple experiments confirmed that CTLs have high basal serine phosphorylation and TCR triggering modifies approximately 20% of these serine phosphorylations. A full list of the basal and TCR regulated serine-threonine phosphorylations identified in at least 3 out of 4 experiments is shown in the supplementary data (see full list in Supplementary Table 2). We also used the Ingenuity program to perform a canonical pathway analysis and molecular and cellular function pathway analysis on the 742 consistent phosphorylations on 473 proteins identified in the CTLs (Fig. 2a). This analysis indicated that the CTL phospho-proteome was significantly overrepresented by proteins that control RNA post-transcriptional modifications, protein synthesis, cell death, gene transcription and polymerization of actin (listed by groups in Supplementary Fig. 3a,b). TCR triggering consistently changed 94 phosphorylations on 81 proteins (including both upregulated and downregulated phosphorylations), representing approximately 17% of all phosphorylated proteins found in our screen (**Tables** 2, 3). Bioinformatics was used to assign the kinases most likely to phosphorylate the CTL phosphoproteins (Fig. 2c and Table 4) and indicated activity of a minimum of at least 18 serine-threonine kinases in CTLs.

Phosphorylated Chromatin regulators in CTLs

One challenge with any screen is how to choose targets for validation. However, in the current experiments we initially focused on transcriptional regulators, as these were significantly overrepresented in the phosphoproteomic screens (Fig. 2a). The full list of this group (Supplementary Fig. 3b) includes transcription factors, coactivators, DNA helicases and histone deacetylases. We noted however that a subset of this list included molecules identified as regulators of chromatin (Table 5). In this context it is well known that the fate of any cell is determined by epigenetic regulation of gene loci. However, the molecular details of chromatin regulation in CTLs are poorly understood but clearly critical to understand how CTLs maintain their effector status. We therefore considered all the chromatin regulators found in the phosphoproteomic screens in CTLs. We did not focus only on TCR-regulated phosphoproteins but also considered basally phosphorylated chromatin regulators as these would be the molecules most likely to offer key insights about the control of CTL differentiation. In this context, there was a consistent identification of the class I histone deacetylases HDAC1 and 2 and the class IIa histone deacetylase HDAC7 as proteins that were constitutively phosphorylated in CTLs (Table 5). These data were striking because the selective control of histone acetylation underpins epigenetic regulation in all cells. In particular, histone acetylation destabilizes the nucleosome structure by neutralizing

the positive charged lysine residues of the N-terminal tail domain of core histones22. The level of histone acetylation is regulated by the antagonistic activity of two groups of enzymes, histone acetyltranferases and histone deacetylases, where HDACs promote chromatin condensation and transcriptional repression.

The identification of HDAC1 and HDAC7 as proteins that were constitutively phosphorylated in CTLs was notable because HDAC1 phosphorylation controls its enzymatic activity23 and HDAC7 phosphorylation controls its intracellular localization and transcriptional repressor function24-31. Moreover, there has been considerable analysis of HDAC7 phosphorylation during thymus development and in the DT40 B lymphoma cell line DT40 (refs.25-27,32). The current paradigm for HDAC7 regulation is that prior to antigen receptor triggering, non-phosphorylated HDAC7 localizes to the nucleus and represses gene transcription33. HDAC7 can function independently of its own intrinsic deacetylase activity and works by forming gene repressive complexes on chromatin34. In contrast, phosphorylated HDAC7 is exported from the nucleus to the cytosol to dock with 14-3-3 proteins. The cytosolic retention of phosphorylated HDAC7 thus relieves the repressive actions of this class IIa HDAC on chromatin25-28,35,36. It was not previously appreciated that HDAC7 is expressed in CTLs and it was particular striking that our screen identified HDAC7 as a CTL protein that is not antigen receptor regulated, rather it was constitutively phosphorylated on S178, S204 and T342; phosphorylation sites known to control nuclear cytoplasmic shuttling of this molecule25,28,36. These data raise the possibility that HDAC7 controls the CTL transcriptional program. We therefore opted to design experimental strategies that would allow us to validate the HDAC7 phosphorylation data and to probe the role of HDAC7 in CTLs.

Constitutive 14-3-3 binding of HDAC7 in CTLs

The HDAC7 phosphorylations identified in the HILIC-IMAC SILAC analyses of CTLs predict that HDAC7 purified from CTLs would constitutively bind 14-3-3 proteins. To explore this possibility we used 14-3-3 affinity purification and SILAC-mass spectrometry analysis to accurately identify and quantify HDAC7-14-3-3 associations (see Supplementary Methods and37). HDAC7 was consistently identified in the 14-3-3 complexes purified from control and TCR-triggered CTLs; there was no effect of TCR triggering on the 14-3-3 binding of HDAC7 (Table 6). We also did a peptide *de novo* synthesis of the acquired pseudo MS^3 spectra for the three HDAC7 peptides purified on the 14-3-3 complexes; KTVpS(178)EPNLK, KEpS(204)APPSLR and pT(342)RSEPLPPSATASPLLAPLQPR (Fig. 3a). The acquired m/z values of the peptide fragments of the according parental ion after collision induced fragmentation (CID) allowed the identification of the peptide sequence and supported HDAC7 S178 and S204 as correctly assigned phosphorylation sites. The data to support HDAC7 T342 phosphorylation were more equivocal. The b_4* and the y_{18} ion of TRSEPLPPSATASPLLAPLQPR (Fig. 3a) were identified indicating that the phosphorylated site was N-terminal of the glutamic acid residue at position 4 of the peptide. However, there was no fragment ion signal closer to the N-terminus than b_4* and y_{18} making a phosphorylation of S344 and T342 equally likely. However, RS (arginine-serine) sequences are known to be resistant to cleavage by trypsin arguing that the actual site of phosphorylation would be S344 rather than T342. In this respect, previous studies have identified S344 rather than T342 as a phosphorylation site in HDAC7 (refs.25,28).

Interestingly, one other class IIa histone deacetylase, HDAC4, was identified in the 14-3-3-complexes purified from CTL lysates but was not found consistently in the phosphopeptide enrichment protocols. One explanation for this discrepancy is that the peptide enrichment on the 14-3-3 complexes enabled detection of less abundant proteins. Spectral counting, which quantifies the total number of MS/MS spectra for peptides from a single protein, can be used quantify the relative abundance of proteins38. There is thus a higher probability that

peptides derived from an abundant protein will lead to a MS/MS event than those derived from less abundant proteins. A spectral count accordingly provides a reliable quantitative assessment of protein abundance. A spectral analysis of the MS/MS events for HDAC4 and HDAC7 from three independent 14-3-3 affinity purifications is shown in Fig. 3b. The data show that HDAC7 was at least 10 times more abundant than HDAC4 in CTLs. Collectively the data show that HDAC7 was the predominant class II HDAC in CTLs and was constitutively phosphorylated on serines 178, 204 and 344 and could constitutively dock with 14-3-3 complexes.

HDAC7 is constitutively localized to the cytosol of CTLs

A distinctive feature of class IIa HDACs is their ability to shuttle between the nucleus and the cytosol. Nucleocytoplasmic shuttling is controlled by interplay between an N-terminal nuclear localization sequence and a C-terminal leucine-rich nuclear export signal, a putative CRM1 recognition sequence30. What is relevant to the present data is that phosphorylation of HDAC7 on the N-terminal sites identified herein directs HDAC7 nuclear export24. The phosphorylation of HDAC7 on the residues identified in Fig. 3 would therefore be predicted to cause HDAC7 to accumulate in the CTL cytosol. To probe the intracellular localization of endogenous HDAC7 in CTLs we initially performed immunoblot analysis of cytosolic and nuclear extracts of CTLs with a pan HDAC7 antisera and a phospho-specific HDAC antisera that can cross-react with HDAC7 molecules phosphorylated on serine 178. Endogenous HDAC7 was constitutively phosphorylated on serine 178 and localized in the cytosol of unstimulated and TCR or phorbol ester activated CTLs (Fig. 4a). To further investigate the subcellular localization of HDAC7, we retrovirally transduced CTLs with a green fluorescent protein (GFP)-tagged fusion protein of HDAC7 (GFP-HDAC7). Immunoblot analysis indicated that GFP-tagged HDAC7 was phosphorylated and localized to the cytosol in CTLs and was able to constitutively bind to 14-3-3 complexes (Fig. 4b).

One question we considered was whether the pattern of HDAC7 localization in the P14 TCR CTLs was universal. To address this issue we examined HDAC7 subcellular localization in other T cell populations. The data (Figure 4c) show that HDAC7 was restricted to the cytosol of CTL expressing a TCR recognizing the ovalbumin-derived peptide SIINFEKL. CTLs produced by polyclonal activation also express HDAC7 in the cytosol (Fig. 4c). Moreover the cytosolic localization of HDAC7 was not restricted to activated T cells: naïve $CD4^+$ and $CD8^+$ T cell populations also localize HDAC7 to the cytosol (Fig. 4d).

Importantly, the constitutive cytosol location of GFP-HDAC7 was confirmed by confocal imaging analysis of CTLs (Fig. 4e). The nuclear export of phosphorylated class II HDACs can be regulated by the CRM1 transporter39. We therefore considered whether the cytosolic localization of HDAC7 in T cells was static or dynamic and caused by the constant export of HDAC7 from the nucleus. To discriminate between these two possibilities, GFP-HDAC7 expressing CTLs were treated with leptomycin B, which efficiently blocks CRM1 transporter function. Treatment of CTLs with leptomycin B caused a time-dependent nuclear accumulation of HDAC7; within 3 hours of leptomycin B treatment, the entire pool of HDAC7 recycled from the cytosol to the nucleus (Fig. 4f). Hence HDAC7 cytoplasmic retention in CTLs is dynamic, not static and is mediated by an active LMB-sensitive nuclear export mechanism.

The role of HDAC7 nuclear exclusion in CTLs

How important is the nuclear exclusion of HDAC7 for the biology of CTLs? To explore this issue we examined the impact of expressing an HDAC7 phosphorylation mutant (GFP-HDAC7-ΔP) in CTLs25,28,35,39. This mutant has been used previously to probe the HDAC7 regulated transcriptional program36. Confocal imaging analysis revealed that GFP-

HDAC7-ΔP localizes to the nucleus of CTLs in contrast to the clear cytoplasmic localization of the wild-type HDAC7 (Fig. 5a,b, compared with Fig. 4e,f). One initial insight of the impact of returning HDAC7 to the nucleus came from flow cytometry experiments to probe the infection efficiency of the viruses encoding GFP-HDAC7-ΔP constructs. CTLs are normally large proliferating cells but analysis by flow cytometry of the FSC-H profile (a relative estimate of cell size) revealed that CTLs expressing GFP-HDAC7-ΔP were smaller (Fig. 5c) as compared to cells expressing wild-type GFP-HDAC7 or to non-transduced cells within the same culture. It also proved impossible to clonally expand CTLs transduced with the mutant HDAC7. We therefore directly quantified the impact of expression of GFP-HDAC7-ΔP on CTL proliferation. CTLs transduced with GFP-HDAC7-ΔP survived but did not undergo normal IL-2 mediated proliferative expansion (Fig. 5d). Hence the nuclear export of HDAC7 is required to maintain CTL size and proliferative capacity.

To explore the molecular basis for the role of HDAC7 in CTLs, we used Affymetrix microarray analysis to explore the impact of GFP-HDAC7-ΔP expression on the CTL transcriptional profile. Approximately 12,000 annotated genes were expressed in CTLs, and the impact of returning HDAC7 to the nucleus was a decrease in the expression of less than 2.5% of these and an increase in the expression of another 6% (Fig. 5e). The inhibitory effect of the HDAC7 mutant was thus quite selective and limited to a small subset of the T cell transcriptome (Fig. 5e, Supplementary Table 3). However, one striking observation was that GFP-HDAC7-ΔP selectively repressed expression of mRNA encoding CD25, a key subunit of the high-affinity receptor for IL-2 (Table 7). The selectivity of this effect of GFP-HDAC7-ΔP mutant on the T cell transcriptome was demonstrated by the fact that it down-regulated expression of CD25 mRNA without impacting on expression of mRNA encoding other key cytokine receptors (Table 7). The effect of GFP-HDAC7-ΔP on the expression CD25 was verified by quantitative PCR analysis (Fig. 6a). Moreover, flow cytometric analysis of CD25 protein expression on GFP-HDAC7-ΔP expressing CTLs versus controls cells (GFP-negative or expressing wild-type HDAC7) revealed that expression of the HDAC7 phospho-mutant causes a reduction in CD25 protein expression on CTLs (Fig. 6b,c).

The strength and duration of IL-2 signaling is known to determine CTL differentiation and proliferation16,17 and the ability of antigen-primed CTLs to respond to IL-2 is dependent on these cells expressing a high-affinity receptor for IL-2 comprising CD25, CD122 and the gamma common chain. In particular, CD25 expression is rate-limiting for CTL responsiveness to IL-2 (refs.16,17). The inability of GFP-HDAC7-ΔP expressing CTLs to proliferate would thus be caused by the reduced expression of CD25. In this context it is important to note that CD25 expression was not completely obliterated by GFP-HDAC7-ΔP. In particular, CTLs expressing the mutant HDAC7 had sufficient IL-2 signaling to survive. The cells thus showed no increased expression of mRNA encoding pro-apoptopic molecules or loss of mRNA encoding survival molecules (Table 8).

High and prolonged expression of CD25 is required to maintain CTL effector function16,17. Accordingly, CTLs with low CD25 expression did not produce the effector cytokine interferon-γ (IFN-γ) in response to antigen receptor triggering (Figs. 6d,e). Moreover, increasing CD25 expression was accompanied by an increased ability to produce IFN-γ in response to antigen receptor triggering (Fig. 6d,e). These data raised the possibility that that expression of HDAC7 phospho-mutant, which downregulated CD25 expression, might impact on antigen receptor-mediated responses of CTLs. We therefore examined the impact of HDAC7 nuclear localization on the ability of CTLs to respond to antigen. CTLs that expressed GFP-HDAC7-ΔP failed to produce IFN-γ when challenged by TCR triggering with cognate peptide (Fig. 6f). Importantly, this effect was cell autonomous as the inhibitory effect of the HDAC7 mutant was restricted to cells that expressed the mutant and there was

no “cross” inhibition of wild-type CTLs, that is non virally transduced CTLs present in the cell cultures. These data show that although HDAC7 phosphorylation and nuclear exclusion is not controlled by the TCR, it is involved in a regulatory process that can dictate the ability of T cells to mediate effector function in response to TCR triggering.

DISCUSSION

The present data report a high resolution mass spectrometry analysis of a cytotoxic T cell serine-threonine phosphoproteome. The results reveal a complex network of protein phosphorylation in CTLs prior to TCR engagement and show that TCR triggering perturbs this network: both increasing and decreasing phosphorylation of proteins with diverse functions in CTLs. One over-represented group of phosphoproteins found in the phosphoproteomic screen was transcriptional regulators. This subset included chromatin regulators notably the histone deacetylases HDAC1, 2, 4 and HDAC7. In the present study we focused on validating the HDAC7 data and established that CTLs have high expression of this class IIa HDAC. Importantly, there is a constitutive signaling pathway maintaining HDAC7 phosphorylation in CTLs that was independent of TCR triggering. HDAC7 phosphorylation ensured constant induce nuclear export of this transcriptional repressor. This process is essential to sustain high expression of CD25 in CTLs and hence is necessary for IL-2-mediated cell growth and proliferation of CTLs. The nuclear export of HDAC7 is also required for CTLs to respond to cognate antigen and produce the effector cytokine IFN-γ. The present results thus show that pathways of protein phosphorylation that are organized prior to TCR engagement can dictate the ability of T cells to mediate effector function in response to TCR triggering. In particular, basal non-TCR regulated pathways of serine-threonine phosphorylation target a key histone deacetylase in CTLs and control expression of genes encoding cytokines, cytokine receptors and adhesion molecules that determine CTL function.

The high basal phosphorylation and nuclear exclusion of HDAC7 in CTLs, in particular the absence of any TCR regulation of HDAC7 in CTLs, is strikingly different to what is known about HDAC7 regulation in the thymus. In these immature cells, HDAC7 phosphorylation and nuclear exclusion is controlled by the TCR25. The phosphorylation of HDAC7 is mediated by the balanced activity of kinases and phosphatases. HDAC kinases include protein kinase C delta, protein kinase Ds, calcium-calmodulin dependent kinases and the AMPK family kinase Mark2 (ref.40). On the other hand, myosin phosphatase and protein phosphatases 2A have been characterized as HDAC7 phosphatases41,42. The constitutive phosphorylation of HDAC7 in CTLs is thus a strong indication that CTLs have high basal activity of one or more of the HDAC kinases and low activity of the phosphatases. In this respect, AMPK family kinases are active in CTLs and important for CTL function as indicated by the fact that deletion of LKB1, which phosphorylates and activates AMP family kinases such as Mark2, causes CTLs to atrophy and die43. Other important insights about potential HDAC7 kinases in CTLs came from using bioinformatics to predict what kinases are active in CTLs. In this analysis, the known substrate specificities of serine-threonine kinases were used to assign the kinase most likely to phosphorylate the sites identified in the CTL mass spectrometry experiments. This modeling concludes that at least 18 different serine-threonine kinases are active in CTLs, including AGC family kinases such as protein kinase A or PKB. This conclusion was reassuring because it is known that PKB is active in CTLs and has a key role to control effector function of these cells5. Similarily, the cytokine-induced protein kinases PIM1/2 were predicted to be active in CTLs, which is consistent with the known pattern of expression of these cytokine-induced protein kinases that function to control cell survival in T cells44. In the context of HDAC7, the modeling indicates that CTLs have high basal activity of calcium-calmodulin dependent kinases and PKD, both of which can phosphorylate class II HDACs45.

The present study focused on chromatin regulators but there were other novel insights about how protein phosphorylation might control T cell biology. For example, the realization that major targets of serine-threonine kinases in T cells were proteins that control RNA stability, RNA cap methylation and protein synthesis was insightful because the ability of CTLs to maintain high-level protein synthesis will be core to the maintenance of CTL effector function. The present study focused on a phosphorylation pathway in CTLs that was not TCR-regulated. However, within the data set there were novel insights about how the TCR acts as an on/off switch to control CTL function. Hence major targets for TCR regulated serine-threonine kinases are proteins that control the actin and microtubule cytoskeleton such as cofilin and stathmin20,21. The present data also show that triggering of the TCR in CTLs causes rapid dephosphorylation of NFATc2; a process known to cause NFAT to translocate to the nucleus where it controls expression of cytokine genes19. In terms of more novel perceptions the data show that CTLs express the transcription coregulator TRIM28 molecules phosphorylated on Serine 473. Moreover, TCR triggering reproducibly increased phosphorylation of TRIM28 Ser473. TRIM28 controls gene expression and chromatin remodeling at specific loci by association with members of the heterochromatin protein 1 (HP1) family and various other chromatin factors. In embryonic stem cells TRIM28 phosphorylation controls pluripotency46 and importantly, the phosphorylation of Ser473 in TRIM28 has been shown to inhibit HP-1 binding and the co-repressor function of TRIM28 (ref.47). The ability of the TCR to direct phosphorylation of TRIM28 on Ser473 thus gives some new ideas as to how the TCR might control gene transcription in CTLs.

In summary, the present study has identified a large number of phosphorylations in CTLs and reveal how phosphoproteomic analysis can direct targeted hypothesis driven experiments that inform about the molecular mechanisms that control T cell function. It should be emphasized that although the present experiments have identified several thousand previously unknown phosphopeptides in a CTL population this is probably not a complete coverage of the CTL phosphoproteome. Hence, tryptic phosphopeptides that are not stable or of the appropriate mass to be identified by mass spectrometry will be missed. Moreover, mass spectrometry favors the identification of either abundant proteins or proteins phosphorylated at high stoichiometry. However, despite this proviso the current experiments have unmasked the complexity of the T cell phosphoproteome and revealed how a basal network of protein phosphorylation maintains transcriptional programs that are permissive for T cell function. The current focus was on CTLs but the concepts will be more generally applicable and indicative of the complexity of the phosphoproteome of all lymphocyte subpopulations. Indeed, a future challenge will be to compare the phosphoproteomes of different lymphocyte subsets to gain insights about the intrinsic and TCR regulated signaling pathways that control T cell function.

Supplementary Material

Refer to Web version on PubMed Central for supplementary material.

Acknowledgments

This project was supported by a Wellcome Trust Principal Research Fellowship and Program grant (065975/Z/01/A). JG was supported by an MRC PhD studentship. We thank members of the Biological Services Unit, R. Clarke of the Flow Cytometry Facility and members of the Cantrell laboratory for critical reading of the manuscript. We thank the Finnish DNA Microarray Centre at the Centre for Biotechnology, Turku, Finland, and N. Schurch for the microarray analysis.

Appendix

METHODS

Mice and SILAC cell culture

P14-LCMV TCR transgenic, OT1-TCR transgenic and C57BL/6 (wild-type) mice were bred and maintained in the WTB/RUTG, University of Dundee in compliance with UK Home Office Animals (Scientific Procedures) Act 1986 guidelines.

P14-LCMV CTL were generated as described5,15 and cultured in SILAC medium (Dundee Cell Products) after 48h of gp33-41 LCMV. The following arginine and lysine isotopes were used:

R0K0:L-[$^{12}C_6$, $^{14}N_4$]arginine (R0) and L-[$^{12}C_6$, $^{14}N_2$]lysine (K0)

R6K4:L-[$^{13}C_6$,$^{14}N_4$]arginine (R6) and L-[$^{12}C_6$, $^{2}H_4$, $^{14}N_2$]lysine (K4)

R10K8: L-[$^{13}C_6$, $^{15}N_4$]arginine (R10) and L-[$^{13}C_6$, $^{15}N_2$]lysine (K8)

After 4 days cells were stimulated with gp33-41 peptide. Cells were combined, lysed and used for 14-3-3 purifications or phosphopeptide enrichment. Details of the materials and methods used can be found in Supplementary Methods.

OT1 and polyclonal CTLs spleens were generated and cultured as the P14-LCMV CTLs, using SIINFEKL peptide for the initial activation of OT1-TCR transgenic cells, or anti-CD3 (2C11) to activate polyclonal, non-TCR transgenic cells.

Phosphopeptide enrichement

Lysates were precipitated with 10% v/v final trichloracetic acid. LysC endopeptidase was added for 4h, followed by trypsin incubation at 30 °C/12h. The proteolytic digests were desalted on C_{18} SepPak cartridges, fractionated by HILIC and fractions collected were enriched using IMAC resin (Phos-Select, Sigma) as described48.

14-3-3 Affinity Purification and proteolytic digestion of proteins ‘in gel’

14-3-3 purifications were performed as described37. *S.cerevisiae* 14-3-3 isoforms BMH1 and BMH2 were coupled to Activated CH-Sepharose 4B (Roche). Lysates and 14-3-3 beads were incubated 1h/4°C. 14-3-3 affinity enriched proteins were separated on a SDS-PAGE and stained with Colloidal Coomassie blue (Invitrogen).

Liquid Chromatography – Mass Spectrometry (LC-MS)

The peptide mixture was separated by nanoscale C_{18} reverse-phase liquid chromatography (Ultimate 3000 nLC (Dionex)) coupled to LTQ-Orbitrap mass spectrometer (LTQ-Orbitrap XL for experiments 1, 2, 3 and LTQ-Orbitrap Velos for experiment 4; Thermo Fisher Scientific).

Mass Spectrometric Data Analysis by MaxQuant

MaxQuant version 1.0.13.1349 was used to process Raw MS spectra. The derived peak list was searched with Mascot demon v.2.2.2 in the Mascot search engine (Matrix Science) against the International Protein Index mouse protein decoy database v.3.52. Phosphopeptide identifications suggested by Mascot were filtered in MaxQuant by applying thresholds on peptide length, mass error, SILAC state, and Mascot score. Ingenuity Pathway Analysis (Ingenuity® Systems, http://www.ingenuity.com) was used to gather information about molecular/ cellular functions.

Cell fractionation, immunoprecipitations and immunoblot analysis

Standard immunoblotting protocols were used5. Cells were washed in cold PBS and resuspended in hypotonic lysis buffer (10 mM HEPES pH 7.9, 15 mM KCl, 4 mM $MgCl_2$, 0.1 mM EDTA, 10 mM NaF, 0.15% NP40, 1 mM PMSF, 1 mM Na_3VO_4, 1 mM DTT), 30×10^6 cells/ml and centrifuged for 1 min/10000*g*. Cytosolic fraction was removed and nuclear/membrane fraction was resuspended in nuclear lysis buffer comprising 10 mM Tris pH 7.05, 50 mM NaCl, 3 0mM Na-pyrophosphate, 50 mM NaF, 5 mM $ZnCl_2$, 10% Glycerol and 0.5% Triton X100. When indicated, cytosolic fractions were immunoprecipitated with GFP antibodies (4E12/8, Cancer Research UK antibody facility) and protein-G-sepharose beads (GEHealthcare). Blots were probed with specific antibodies for HDAC7 (H-273, Santa Cruz Biotechnology), phospho Erk1/2 (E-10, Cell Signalling), IκBα (C-21, Santa Cruz Biotechnology), SCM1 (A300-055A, Bethyl) or GFP (3E1, CRUK antibody facility).

Generation of phospho-specific HDAC7 antibody

Phosphopeptide corresponding to pS251 in mHDAC5 (conserved in mHDAC7 pS178) PLRKTApSEPNLKV was synthesized, coupled to KLH and used to generate a rabbit antibody specific for anti-phospho-HDAC7 using standard immunization techniques. The resulting antisera were screened for antigen reactivity by ELISA and immunoblot analysis (see Supplementary Figure 4 and data not shown).

Purification of naïve T cells

Spleens and lymph nodes were harvested, disaggregated and pooled. $CD4^+$, $CD8^+$ or total T cells were purified by negative selection using, respectively, $CD4^+$-, $CD8^+$- and Pan-T Cell Isolation kit by magnetic cell sorting (AutoMacs, Miltenyi Biotec).

Retrovirus production and CTL transduction

GFP-HDAC732 was subcloned in to pBMN-Z retroviral vector (Addgene). GFP-HDAC7-ΔP triple mutant S178A/S344A/S479A was obtained from the College of Life Sciences Cloning Service using QuickChange mutagenesis kit (Stratagene) and subcloned in pBMN vector. Constructs were verified by sequencing. Retrovirus production and CTL transduction was performed as described5.

Confocal microscopy

Cells were adhered to poly-L-Lysine (Sigma-Aldrich) coated coverslips, fixed with 4% paraformaldehyde for 30 min/25°C. When indicated, cells were stained with DAPI (Invitrogen). Confocal microscopy was performed in Zeiss LSM700 confocal microscope using an alpha Plan-Fluar 100× objective (numerical aperture 1.45).

Flow cytometry analysis

Cells were stained as described5. CD25-FITC (7D4), CD25-PE (PC61), CD2-PE (RM2-5), CD69 (H1.2F3), CD5-PE (53-7.3) and IFN-γ-APC (XMG1.2) were from BD Pharmingen. For IFN-γ intracellular staining, cells were TCR stimulated for 4 h in presence of BD-Golgi-Plug (BD Biosciences), and processed using IC Fixation and Permeabilization buffers (eBiosciences) following manufacture's instructions. Data were acquired on a FACSCalibur (Becton Dickinson) flow cytometer and analyzed using FlowJo software (Treestar).

Affimetrix GeneChip mouse genome array

CTLs retrovirally transduced with GFP-HDAC7-ΔP vector were sorted using a FACS Vantage (Becton Dickinson) cell sorter to obtain GFP− (control cells) and GFP+ (GFP-HDAC7-ΔP). Cell sorting was performed in three independent replicates, RNA was

extracted as described below and microarray analysis was performed by the Finnish DNA Microarray Centre at the Centre for Biotechnology, Turku, Finland, using GeneChip mouse genome 430_2.0 array (Affimetrix). Affymetrix Expression Console v1.1 (Affimetrix) was used to normalise the data. MAS5 normalization was used to select the probes present in at least one sample and RMA was used to normalize data. Further statistical analysis was performed using Multiple Experiment Viewer v4.3 (www.TM4.org). 2 fold or more differences in GFP+ vs GFP− cells were identified with the SAM algorithm50, setting the 90th percentile false discovery rate to 5%. Identification of the annotated genes was performed using the Database for Annotation, Visualization and Integrated Discovery (DAVID v6.7)51. The data discussed in this publication have been deposited in NCBI's Gene Expression Omnibus52 and are accessible through GEO Series accession number GSE27092 (http://www.ncbi.nlm.nih.gov/geo/query/acc.cgi?acc=GSE27092).

Quantitative real-time PCR

RNA was extracted using RNeasy Mini kit (QIAGEN) and reverse-transcribed using qScript cDNA synthesis kit (Quanta BioSciences) according to manufacturer's protocol. Quantitative PCR was performed in 96-well plate using iQ SYBR Green based detection on a Bio-Rad iCycler (Bio-Rad Laboratories). 18S mRNA abundance was used for normalization and derived values averaged. Primers: 18s-forward: 5′-ATCAGATACCGTCGTAGTTCCG-3′, 18s-reverse:5′-TCCGTCAATTCCTTTAAGTTTCAGC-3′, CD25-forward: 5′-TTTCCTTCTGATCCCTGGGTTTC-3′, CD25-reverse: 5′ GATAGAGTTGCTGTTATGTCCTGTG-3′.

REFERENCES

1. Matthews SA, Cantrell DA. New insights into the regulation and function of serine/threonine kinases in T lymphocytes. Immunol Rev. 2009; 228:241–252. [PubMed: 19290932]
2. Lin JX, Spolski R, Leonard WJ. Critical role for Rsk2 in T-lymphocyte activation. Blood. 2008; 111:525–533. [PubMed: 17938253]
3. Salmond RJ, Emery J, Okkenhaug K, Zamoyska R. MAPK, phosphatidylinositol 3-kinase, and mammalian target of rapamycin pathways converge at the level of ribosomal protein S6 phosphorylation to control metabolic signaling in CD8 T cells. J Immunol. 2009; 183:7388–7397. [PubMed: 19917692]
4. Sinclair LV, et al. Phosphatidylinositol-3-OH kinase and nutrient-sensing mTOR pathways control T lymphocyte trafficking. Nat Immunol. 2008; 9:513–521. [PubMed: 18391955]
5. Waugh C, Sinclair L, Finlay D, Bayascas JR, Cantrell D. Phosphoinositide (3,4,5)-triphosphate binding to phosphoinositide-dependent kinase 1 regulates a protein kinase B/Akt signaling threshold that dictates T-cell migration, not proliferation. Mol Cell Biol. 2009; 29:5952–5962. [PubMed: 19703999]
6. Rao RR, Li Q, Odunsi K, Shrikant PA. The mTOR kinase determines effector versus memory CD8+ T cell fate by regulating the expression of transcription factors T-bet and Eomesodermin. Immunity. 32:67–78. [PubMed: 20060330]
7. Araki K, et al. mTOR regulates memory CD8 T-cell differentiation. Nature. 2009; 460:108–112. [PubMed: 19543266]
8. Pearce EL, et al. Enhancing CD8 T-cell memory by modulating fatty acid metabolism. Nature. 2009; 460:103–107. [PubMed: 19494812]
9. Finlay DK, et al. Phosphoinositide-dependent kinase 1 controls migration and malignant transformation but not cell growth and proliferation in PTEN-null lymphocytes. J Exp Med. 2009; 206:2441–2454. [PubMed: 19808258]
10. Ong SE, et al. Stable isotope labeling by amino acids in cell culture, SILAC, as a simple and accurate approach to expression proteomics. Mol Cell Proteomics. 2002; 1:376–386. [PubMed: 12118079]

11. Brockmeyer C, et al. T cell receptor (TCR)-induced tyrosine phosphorylation dynamics identifies themis as a new TCR signalosome component. J Biol Chem. [PubMed: 21189249]
12. Mayya V, et al. Quantitative phosphoproteomic analysis of T cell receptor signaling reveals system-wide modulation of protein-protein interactions. Sci Signal. 2009; 2:ra46. [PubMed: 19690332]
13. Nguyen V, et al. A new approach for quantitative phosphoproteomic dissection of signaling pathways applied to T cell receptor activation. Mol Cell Proteomics. 2009; 8:2418–2431. [PubMed: 19605366]
14. Cornish GH, Sinclair LV, Cantrell DA. Differential regulation of T-cell growth by IL-2 and IL-15. Blood. 2006; 108:600–608. [PubMed: 16569767]
15. Weninger W, Crowley MA, Manjunath N, von Andrian UH. Migratory properties of naive, effector, and memory CD8(+) T cells. J Exp Med. 2001; 194:953–966. [PubMed: 11581317]
16. Kalia V, et al. Prolonged interleukin-2Ralpha expression on virus-specific CD8+ T cells favors terminal-effector differentiation in vivo. Immunity. 32:91–103. [PubMed: 20096608]
17. Pipkin ME, et al. Interleukin-2 and inflammation induce distinct transcriptional programs that promote the differentiation of effector cytolytic T cells. Immunity. 32:79–90. [PubMed: 20096607]
18. Malek TR, Castro I. Interleukin-2 receptor signaling: at the interface between tolerance and immunity. Immunity. 33:153–165. [PubMed: 20732639]
19. Muller MR, Rao A. NFAT, immunity and cancer: a transcription factor comes of age. Nat Rev Immunol. 10:645–656. [PubMed: 20725108]
20. Wabnitz GH, Nebl G, Klemke M, Schroder AJ, Samstag Y. Phosphatidylinositol 3-kinase functions as a Ras effector in the signaling cascade that regulates dephosphorylation of the actin-remodeling protein cofilin after costimulation of untransformed human T lymphocytes. J Immunol. 2006; 176:1668–1674. [PubMed: 16424196]
21. Marklund U, et al. Serine 16 of oncoprotein 18 is a major cytosolic target for the Ca2+/calmodulin-dependent kinase-Gr. Eur J Biochem. 1994; 225:53–60. [PubMed: 7925472]
22. Wang Z, et al. Genome-wide mapping of HATs and HDACs reveals distinct functions in active and inactive genes. Cell. 2009; 138:1019–1031. [PubMed: 19698979]
23. Pflum MK, Tong JK, Lane WS, Schreiber SL. Histone deacetylase 1 phosphorylation promotes enzymatic activity and complex formation. J Biol Chem. 2001; 276:47733–47741. [PubMed: 11602581]
24. Martin M, Kettmann R, Dequiedt F. Class IIa histone deacetylases: regulating the regulators. Oncogene. 2007; 26:5450–5467. [PubMed: 17694086]
25. Dequiedt F, et al. HDAC7, a thymus-specific class II histone deacetylase, regulates Nur77 transcription and TCR-mediated apoptosis. Immunity. 2003; 18:687–698. [PubMed: 12753745]
26. Dequiedt F, et al. Phosphorylation of histone deacetylase 7 by protein kinase D mediates T cell receptor-induced Nur77 expression and apoptosis. J Exp Med. 2005; 201:793–804. [PubMed: 15738054]
27. Parra M, Kasler H, McKinsey TA, Olson EN, Verdin E. Protein kinase D1 phosphorylates HDAC7 and induces its nuclear export after T-cell receptor activation. J Biol Chem. 2005; 280:13762–13770. [PubMed: 15623513]
28. Kao HY, et al. Mechanism for nucleocytoplasmic shuttling of histone deacetylase 7. J Biol Chem. 2001; 276:47496–47507. [PubMed: 11585834]
29. Zhang CL, et al. Class II histone deacetylases act as signal-responsive repressors of cardiac hypertrophy. Cell. 2002; 110:479–488. [PubMed: 12202037]
30. McKinsey TA, Zhang CL, Lu J, Olson EN. Signal-dependent nuclear export of a histone deacetylase regulates muscle differentiation. Nature. 2000; 408:106–111. [PubMed: 11081517]
31. McKinsey TA, Zhang CL, Olson EN. Activation of the myocyte enhancer factor-2 transcription factor by calcium/calmodulin-dependent protein kinase-stimulated binding of 14-3-3 to histone deacetylase 5. Proc Natl Acad Sci U S A. 2000; 97:14400–14405. [PubMed: 11114197]
32. Matthews SA, et al. Essential role for protein kinase D family kinases in the regulation of class II histone deacetylases in B lymphocytes. Mol Cell Biol. 2006; 26:1569–1577. [PubMed: 16449666]

33. Martin M, Kettmann R, Dequiedt F. Class IIa histone deacetylases: conducting development and differentiation. Int J Dev Biol. 2009; 53:291–301. [PubMed: 19412888]
34. Fischle W, et al. Enzymatic activity associated with class II HDACs is dependent on a multiprotein complex containing HDAC3 and SMRT/N-CoR. Mol Cell. 2002; 9:45–57. [PubMed: 11804585]
35. Li X, Song S, Liu Y, Ko SH, Kao HY. Phosphorylation of the histone deacetylase 7 modulates its stability and association with 14-3-3 proteins. J Biol Chem. 2004; 279:34201–34208. [PubMed: 15166223]
36. Kasler HG, Verdin E. Histone deacetylase 7 functions as a key regulator of genes involved in both positive and negative selection of thymocytes. Mol Cell Biol. 2007; 27:5184–5200. [PubMed: 17470548]
37. Dubois F, et al. Differential 14-3-3 affinity capture reveals new downstream targets of phosphatidylinositol 3-kinase signaling. Mol Cell Proteomics. 2009; 8:2487–2499. [PubMed: 19648646]
38. Gao J, Opiteck GJ, Friedrichs MS, Dongre AR, Hefta SA. Changes in the protein expression of yeast as a function of carbon source. J Proteome Res. 2003; 2:643–649. [PubMed: 14692458]
39. Gao C, et al. CRM1 mediates nuclear export of HDAC7 independently of HDAC7 phosphorylation and association with 14-3-3s. FEBS Lett. 2006; 580:5096–5104. [PubMed: 16956611]
40. Yang XJ, Seto E. The Rpd3/Hda1 family of lysine deacetylases: from bacteria and yeast to mice and men. Nat Rev Mol Cell Biol. 2008; 9:206–218. [PubMed: 18292778]
41. Parra M, Mahmoudi T, Verdin E. Myosin phosphatase dephosphorylates HDAC7, controls its nucleocytoplasmic shuttling, and inhibits apoptosis in thymocytes. Genes Dev. 2007; 21:638–643. [PubMed: 17369396]
42. Martin M, et al. Protein phosphatase 2A controls the activity of histone deacetylase 7 during T cell apoptosis and angiogenesis. Proc Natl Acad Sci U S A. 2008; 105:4727–4732. [PubMed: 18339811]
43. Tamas P, et al. LKB1 is essential for the proliferation of T-cell progenitors and mature peripheral T cells. Eur J Immunol. 40:242–253. [PubMed: 19830737]
44. Fox CJ, Hammerman PS, Thompson CB. The Pim kinases control rapamycin-resistant T cell survival and activation. J Exp Med. 2005; 201:259–266. [PubMed: 15642745]
45. Chang S, Bezprozvannaya S, Li S, Olson EN. An expression screen reveals modulators of class II histone deacetylase phosphorylation. Proc Natl Acad Sci U S A. 2005; 102:8120–8125. [PubMed: 15923258]
46. Seki Y, et al. TIF1beta regulates the pluripotency of embryonic stem cells in a phosphorylation-dependent manner. Proc Natl Acad Sci U S A. 107:10926–10931. [PubMed: 20508149]
47. Chang CW, et al. Phosphorylation at Ser473 regulates heterochromatin protein 1 binding and corepressor function of TIF1beta/KAP1. BMC Mol Biol. 2008; 9:61. [PubMed: 18590578]
48. McNulty DE, Annan RS. Hydrophilic interaction chromatography reduces the complexity of the phosphoproteome and improves global phosphopeptide isolation and detection. Mol Cell Proteomics. 2008; 7:971–980. [PubMed: 18212344]
49. Cox J, Mann M. MaxQuant enables high peptide identification rates, individualized p.p.b.-range mass accuracies and proteome-wide protein quantification. Nat Biotechnol. 2008; 26:1367–1372. [PubMed: 19029910]
50. Tusher VG, Tibshirani R, Chu G. Significance analysis of microarrays applied to the ionizing radiation response. Proc Natl Acad Sci U S A. 2001; 98:5116–5121. [PubMed: 11309499]
51. Huang da W, Sherman BT, Lempicki RA. Systematic and integrative analysis of large gene lists using DAVID bioinformatics resources. Nat Protoc. 2009; 4:44–57. [PubMed: 19131956]
52. Edgar R, Domrachev M, Lash AE. Gene Expression Omnibus: NCBI gene expression and hybridization array data repository. Nucleic Acids Res. 2002; 30:207–210. [PubMed: 11752295]

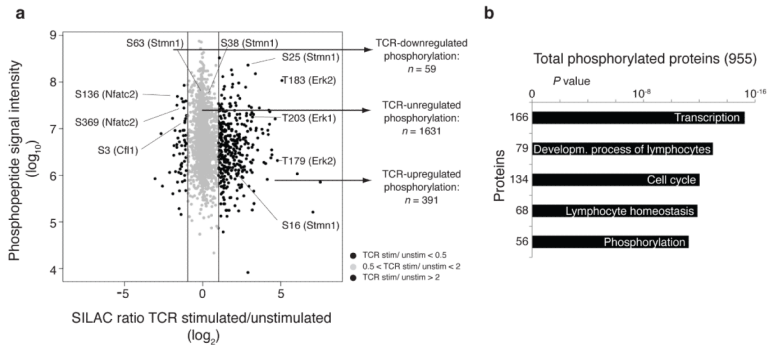

Figure 1.

Analysis of the basal and TCR regulated phosphoproteome in CTLs. P14 LCMV CTLs differentially labeled in SILAC media were either left unstimulated or triggered via their TCR with cognate peptide for 1 h. Cells were lysed and phosphopeptide purification using HILIC/IMAC enrichment was performed as described in Supplementary Methods. The resulting peptides were analyzed and identified using a LTQ-Orbitrap XL via MaxQuant v. 1.0.13.13. **(a)** Graphic shows the ratio/ intensity plot of 2,078 phosphopeptides identified in T cell lysates. TCR downregulated and upregulated phosphorylations are indicated as black dots. Selected proteins that have been previously shown to change phosphorylation after TCR stimulation are indicated. **(b)** All 955 identified phosphoproteins were subjected Ingenuity Pathway Analysis. The result of the molecular and cellular function analysis is shown.

Europe PMC Funders Author Manuscripts

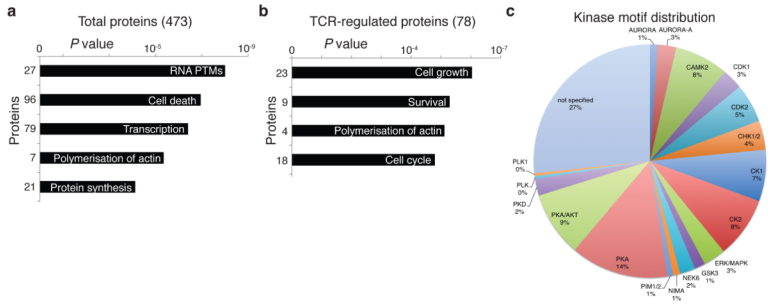

Figure 2.

Ingenuity Pathway Analysis of consistent phosphorylations in CTLs. SILAC and HILIC/IMAC purification protocols were independently performed four times, including amino acid labeling switch. The isotope combination (unstimulated/stimulated) was as follows: experiment 1, R10K8/R0K0 (Fig. 1), experiment 2, R0K0/R6K6, experiment 3 and 4, R0K0/R6K6 (not shown). CTLs were stimulated for 1 h with cognate peptide in experiments 1, 2 and 3 and for 10 min in experiment 4. Reproducible phosphorylations in three out of four experiments were considered for analysis. **(a)** Ingenuity Pathway Analysis of 742 phosphorylations on 473 different proteins found in at least three of the four conducted SILAC experiments. **(b)** Ingenuity Pathway Analysis of TCR-regulated 94 phosphorylations on 78 different proteins consistently found in our screening using 1.5 fold as threshold for regulation. **(c)** Representation of the frequency of kinases predicted to be active in CTL using MaxQuant software analysis. MaxQuant uses a sequence window ± 6 amino acids around the identified phosphorylation site to determine the kinase that could phosphorylate this motif.

Europe PMC Funders Author Manuscripts

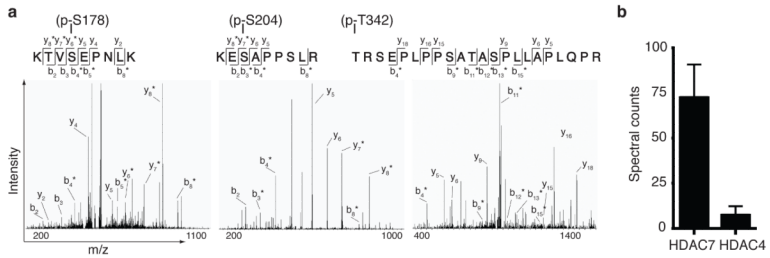

Figure 3.

Phosphorylated chromatin regulators in CTLs: class II histone deacetylase 7 (HDAC7). **(a)** *De novo* synthesis of the acquired pseudo MS^3 spectra in one of the four experiments performed for the three peptides KTVpSEPNLK, KEpSAPPSLR and pTRSEPLPPSATASPLLAPLQPR. * in y and b ion series indicates loss of phosphate. **(b)** Spectral counting of the two detected class IIa HDACs in CTLs, HDAC7 and HDAC4 separately calculated for phosphopeptide enrichment and 14-3-3 affinity purification screens. Graph represents the averaged spectral counts of the four SILAC experiments ± SEM.

Europe PMC Funders Author Manuscripts

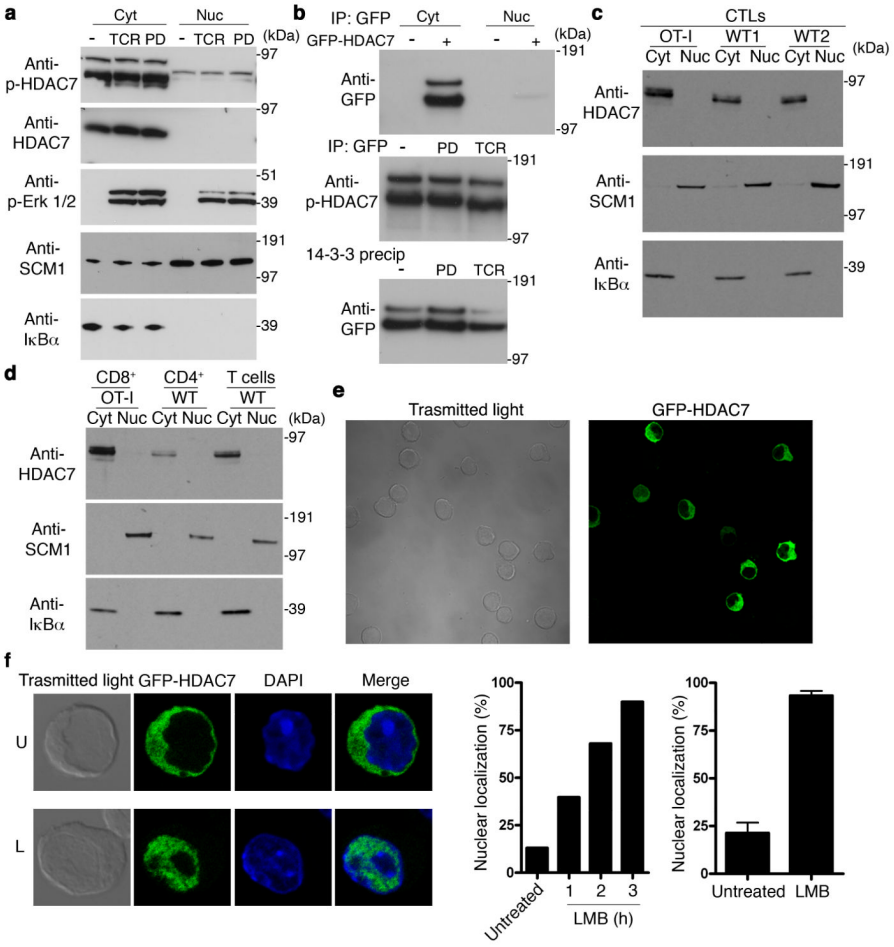

Figure 4.

Subcellular distribution of HDAC7 in CTLs. **(a)** Immunoblot analysis of CTLs cytosolic and nuclear extracts treated with peptide (TCR), PDBu (PD) or untreated (−) for 30 min. Anti-IκBα and anti-SCM1 were included as controls for fraction purity and anti-p-Erk as activation control. Representative of 3 experiments. **(b)** Immunoblot analysis of CTLs retrovirally transduced with GFP-HDAC7. (Top) cytosolic and nuclear extracts from GFP-HDAC7 transduced (+) or non-transduced (−) were immunoprecipitated and immunoblotted with anti-GFP. (Middle, bottom), GFP-HDAC7 transduced CTLs were stimulated with PDBu (PD), peptide (TCR) or unstimulated (−) for 2h. In middle panel, cytosolic extracts were immunoprecipitated with anti-GFP and immunoblotted with anti-p-HDAC7. In bottom panel, cytosolic extracts were affinity purified with 14-3-3-sepharose and immunoblotted with anti-GFP. Data are representative of two experiments. **(c)** Immunoblot analysis of HDAC7 expression in cytosolic and nuclear extracts of CTLs obtained from OT1 and two sets of polyclonal, non-TCR-Tg mice (WT). Representative of 2 experiments. **(d)** Immunoblot analysis of HDAC7 expression in cytosolic and nuclear extracts of different populations of naïve T cells: $CD8^+$ cells from TCR-Tg OT1 mice, polyclonal $CD4^+$ and total T cells from non-TCR-Tg (WT). Representative of 2 experiments. **(e)** P14-LCMV CTLs retrovirally transduced with a vector encoding GFP-HDAC7 chimeric protein were analyzed by confocal microscopy. Images are representative of ten independent experiments. **(f)** GFP-HDAC7 expressing P14-LCMV CTLs were left untreated (U) or treated with leptomycin B (L) and stained with DAPI. Images are representative of 3h of

LMB treatment. First graph represents the percentage of cells with nuclear GFP-HDAC7 at different time points of LMB treatment. Second graph represents average ± SEM after 3h of LMB (n=7). At least 100 cells were counted in each experiment and time point.

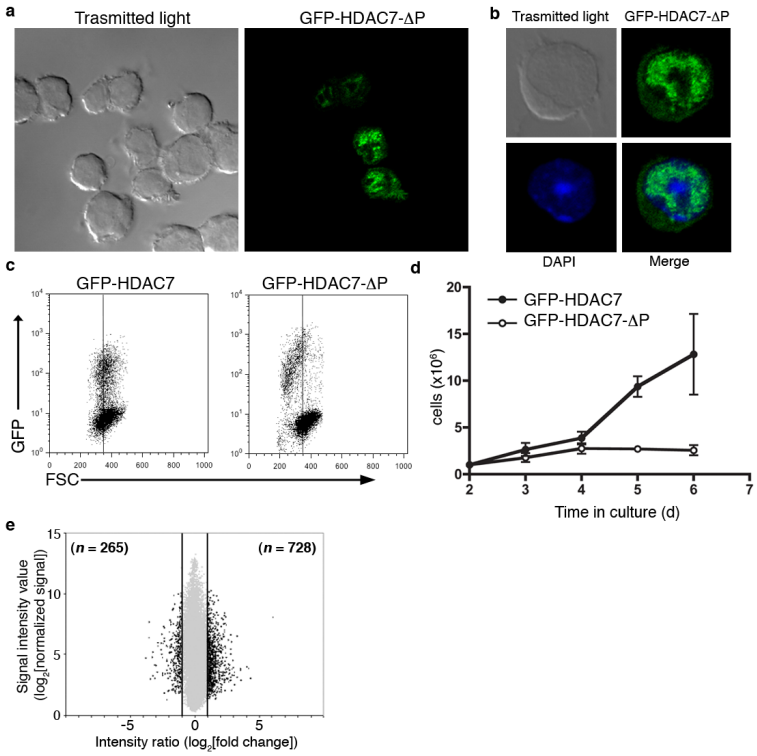

Figure 5.

HDAC7 nuclear exclusion is required for normal CTL function. P14-LCMV CTLs were retrovirally transduced with GFP-HDAC7-ΔP or GFP-HDAC7. In **(a)** and **(b)** subcellular distribution of GFP-HDAC7-ΔP was analyzed by microscopy. In **(b)**, DAPI staining was included. Images are representative of 4 experiments. **(c)** GFP-HDAC7 and GFP-HDAC7-ΔP transduced CTLs were analyzed by flow cytometry. Plots representative of 10 experiments. **(d)** Cell numbers and GFP expression were assessed daily and represented as cell number over time. Graph represents average number ± SEM of 3 experiments. **(e)** GFP-HDAC7-ΔP transduced CTLs were sorted based on GFP expression, and microarray analysis was performed using Affymetrix GeneChip mouse genome 430_2.0 array comparing expression profile of GFP-HDAC7-ΔP (GFP^+) and control (GFP^-) cells. Graph shows the distribution of the intensity ratio (log2 fold change, GFP-HDAC7-ΔP relative to control) plotted by the average of the normalized intensity values for 23,653 probes identified as present in at least one sample. Probes with 2 fold change or higher are represented by black dots (1,457 probes, 993 annotated genes). Grey dots represent probes with no significant change or fold change below 2 fold (22,196 probes, 11,148 annotated genes). Using a 2-fold cut, 265 genes show decreased expression in GFP-HDAC7-ΔP cells, and 728 genes shown increased expression. Data are accessible through GEO Series accession number GSE27092 (http://www.ncbi.nlm.nih.gov/geo/query/acc.cgi?acc=GSE27092).

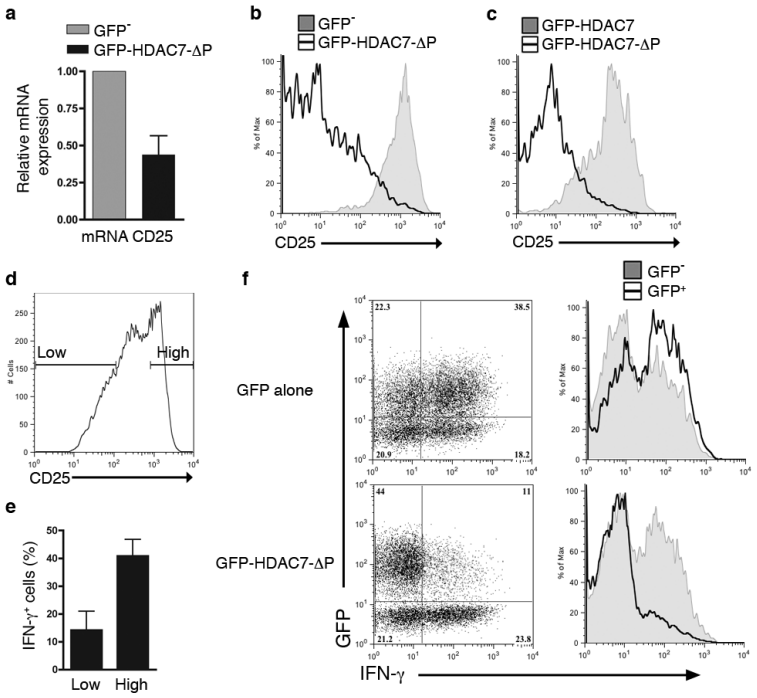

Figure 6.

HDAC7 nuclear exclusion is required for expression of the high affinity IL2 receptor. **(a)** Relative expression of CD25 mRNA in sorted GFP negative (GFP−) and GFP-HDAC7-ΔP. Data shown are an average of three different experiments ± SEM (*AU= arbitrary units). **(b)** GFP-HDAC7-ΔP transduced P14-LCMV CTLs were stained for CD25 and analyzed by flow cytometry. GFP positive and negative cells were electronically gated to compare CD25 expression in both populations. **(c)** GFP-HDAC7 and GFP-HDAC7-ΔP transduced P14-LCMV-CTLs were stained for CD25 and analyzed by flow cytometry. Histograms in **b** and **c** are representative of three independently performed experiments. **(d,e)** P14-LCMV CTLs were stimulated with cognate peptide for 4h before assessing surface CD25 and intracellular IFN-γ expression by flow cytometry. **(e)** Expression of CD25 was electronically gated as in **(d)** to compare IFN-γ expression. The percentage of IFN-γ positive cells in both populations is represented as an averaged value of four experiments ± SEM. **(f)** IFN-γ production was assessed by intracellular staining in P14-LCMV CTLs expressing GFP-HDAC7-ΔP or GFP alone after stimulation with peptide for 4h. Data are representative of three experiments.

Europe PMC Funders Author Manuscripts

Europe PMC Funders Author Manuscripts

Table 1

List of selected phosphopeptides from the 450 TCR regulated phosphorylations previously known to change phosphorylation status after TCR stimulation with the ratio (TCR stimulated/unstimulated) and phosphorylation sites/sequences found in our screening (experiment 1).

Gene name	Protein name	Aa	Position	Ratio (TCR stimulated/ unstimulated)	Sequence Window
Cfl1	Cofilin-1	S	3	0.45	____MASGVAVSD
Mapk3	ERK1	T	203	9.1	DHTGFLTEYVATR
Mapk1	ERK2	T	183	33.5	DHTGFLTEYVATR
		T	179	27.5	DPDHDHTGFLTEY
Nfatc2	NFAT1	S	270	7.29	APLPAASPQRSRS
		S	757	4.6	AALYQRSKSLSPG
		S	238	2.89	SCLGRHSPVPRPA
		S	365	0.56	QEERRNSAPESIL
		S	369	0.43	RNSAPESILLVPP
		S	136	0.33	GRDAGLSPEQPAL
Stmn1	Stathmin	S	25	7.46	AFELILSPRSKES
		S	16	2.35	ELEKRASGQAFEL
		S	38	1.35	VPDFPLSPPKKKD
		S	63	0.90	AEERRKSHEAEVL

Europe PMC Funders Author Manuscripts

Nat Immunol. Author manuscript; available in PMC 2011 October 01.

Table 2

List of 72 phosphorylations consistently (found in at least 3 out of 4 experiments) up-regulated after TCR stimulation with the ratio (TCR stimulated/ unstimulated) and phosphorylation sites/sequences using 1.5 fold as threshold for regulation.

	Ratio (TCR stimulated/ unstimulated)						
Gene Name	**Exp 1**	**Exp 2**	**Exp 3**	**Exp 4**	**Aa**	**Position**	**Sequence Window**
Acly		3.01	4.09	2.21	T	453	TPAPSRTASFSES
Acly	2.96	3.41	3.48	1.78	S	455	APSRTASFSESRA
Add3	2.25		2.77	2.9	S	423	DDSAPLSPLKFMA
Ahnak	1.4	1.9	2.9	1.63	S	136	IKPRLRSEDGVEG
Akt1s1	1.52	1.73		1.53	T	318	PRPRLNTSDFQKL
Ap1gbp1	1.95	2.37	1.39	1.94	S	1067	SHKRSLSLGDKEI
Arhgef7	3.74	4.17	4.32	1.95	S	673	KPERKPSDEEFAV
Bcl2	2.8	2.93		1.77	T	69	RDMAARTSPLRPL
Bmp2k	2.12		2.6	1.67	S	908	LPARPRSVDIFGS
Cblb	2.43		1.52	2.2	S	521	QKGIVRSPCGSPT
Cblb	2.43		1.52	2.2	S	525	VRSPCGSPTGSPK
Cbx5	2.31		2.01	2.44	S	93	GNKRKSSFSNSAD
Ccs	1.85		1.91	1.99	S	267	GQGRKDSAQPPAH
Cenpe	3.17		4.47	3.11	S	2426	FDNRSKSLPAPHP
Dlgap5	1.52	1.59	1.58	1.24	S	328	YQVAPLSPRSANA
Eif4b	1.54	1.82	2.73	1.79	S	425	RTGSESSQTGASA
Eif4b	1.72	2.15	2.73	1.68	T	420	ERERSRTGSESSQ
Eml3		2.27	2.65	1.68	S	177	LSRKAASSANLLL
Evl	2.22	1.91	1.87		S	373	RVKPAGSVNDVGL
Evl	1.19	2.17	2.82	1.85	S	333	RKPWERSNSVEKP
Evl	1.27	2.29	2.09	1.74	S	335	PWERSNSVEKPVS
Fancd2	2.47		4.29	2.22	S	10	KRRRLDSEDKENL
FLJ45252	4.6	3.71	5.35	1.62	S	115	PINQRASDDLGEP
Foxk1	1.82	3.65	3.25	0.75	S	243	PNSCPASPRGAGS

	Ratio (TCR stimulated/ unstimulated)							
Gene Name	Exp 1	Exp 2	Exp 3	Exp 4	Aa	Position	Sequence Window
Grap2	4.75	9.42	10.34	5.37	T	254	LMHRRHTDPVQLQ
Gtse1	1.66		4.11	2.84	S	476	RTHRLQSWTPASR
Hn1	3.19	3.6	4.45		S	87	GTQRSNSSEASSG
Hnrnpa1	1.83	6.49	1.63	1.05	S	6	_MSKSESPKEPEQ
Hnmph1	1.77	2.01	1.75	1.22	S	104	KHTGPNSPDTAND
Ier3	5.9		11.47	1.58	S	31	PELRRGSGPEIFT
IPI00381495.5	1.73		1.76	2.46	S	237	PVSAPPSPRDISM
Lag3	1.82	6.38	1.91	2.88	S	476	LLLRRFSALEHGI
Larp1	2	2.06	2.32	1.55	S	1018	PTTVPESPNYRNA
Lcp1	4.62		6.31	2.31	S	5	__MARGSVSDEEM
Lig1		4.77	6.8	2.08	S	81	KVAQVLSCEGEDE
Lsp1	1.84		2.26	1.61	S	180	DTVELSSPPLSPT
Mcm2	2.8	2.82	2.33	1.44	S	21	RQRRRISDPLTSS
Mki67	3.62		4.4	4.87	S	125	EPSRRASRDSFCA
Mkl1	2.17		2.53	1.7	S	349	APTPSRSLSTSSS
Mll2		1.9	2.1	1.57	S	1969	ASEPLLSPPPFGE
Mycbp2	1.6		1.55	1.63	S	2943	PRERSKSDSYTLD
Myo9b	3.25	2.09	1.97		S	1293	AQDKPESPSGSTQ
Myo9b	3.3	9.98	7.53	2.22	T	1346	ATGAALTPTEERR
Nbn		2.35	2.74	1.64	S	398	QSSRKLSQETFNI
Ncdp1	2.73		3.72	1.62	T	21	PHKRRKTSDANET
Ncdp1	3.44		3.58	1.64	S	22	HKRRKTSDANETE
Pea15		3.62	8.93	2.55	S	116	DIIRQPSEEEIIK
Pkn2	1.51	1.87	2.08	1.23	S	582	APPRASSLGETDE
Pnn	4.21	4.37	4.3	3.92	S	66	LLRRGFSDSGGGP
Ptpn7	7.94	2.78	7.33	2.18	S	143	CLGRAQSQEDSDY
Rab3gap1	3.54	2.62	3.7	1.75	S	536	DEGKKTSLSDSTT

Europe PMC Funders Author Manuscripts

	Ratio (TCR stimulated/ unstimulated)							
Gene Name	Exp 1	Exp 2	Exp 3	Exp 4	Aa	Position	Sequence Window
Ran	8.96		6.5	1.99	S	135	RKVKAKSIVFHRK
Rasal3	0.4	1.9	3.18	1.75	S	885	RAWTRASASLPRK
Rasal3	2.28		2.93	3.82	S	52	GWGRALSHQEPMV
Rbm7	5.11	9.22	6.03	6.66	S	136	MVQRSFSSPEDYQ
Rdbp	2.54		5.06	4.96	S	49	QGGVKRSLSEQPV
Sec22b	1.9		1.51	2.22	S	137	ARRNLGSINTELQ
Sgta	1.89	2.01	1.9	1.95	S	307	VRSRTPSASHEEQ
Snx2	4.73	4.49		2.03	T	104	PAVTPVTPTTLIA
Stmn1	3.19	1.55	2.35	1.29	S	16	ELEKRASGQAFEL
Stmn1	4.99	3.13	7.46	2.26	S	25	AFELILSPRSKES
Tex2	3.13		5.51	1.57	S	269	PSSPLTSPSDTRS
Toe1	3.59		3.65	1.57	S	349	KDKRKRSLQSQPG
Tpd52l2	0.47	1.72	2.21	1.71	S	189	NSATFKSFEDRVG
Trim28	4.82	4.77	3.79		S	471	VSGMKRSRSGEGE
Trim28	4.49	4.81	3.71	1.94	S	473	GMKRSRSGEGEVS
Txlna	2.15	1.6	1.66	1.09	S	523	GAQPASSPRATDA
Uba1	3.23	3.04	2.37	1.46	S	46	GMAKNGSEADIDE
Ubash3a		6.41	5.3	11.2	S	13	QLYAKVSNKLKGR
Ubxn7		2.99	2.74	4.11	S	278	PKKCARSESLIDA
Wipf1	0.4	6.16	2.54	1.7	S	330	LPQRNLSLTSSAP
Zfc3h1	1.18	4.01	2.2	2.35	S	356	NLTRRLSASDIVS

Europe PMC Funders Author Manuscripts

Europe PMC Funders Author Manuscripts

Table 3

List of 22 phosphorylations consistently (found in at least 3 out of 4 experiments) down-regulated after TCR stimulations with the ratio (TCR stimulated/ unstimulated) and phosphorylation sites/sequences using 1.5 fold as threshold for regulation.

	Ratio (TCR stimulated/ unstimulated)						
Gene Name	**Exp 1**	**Exp 2**	**Exp 3**	**Exp 4**	**Aa**	**Position**	**Sequence Window**
Akap13	0.65		0.67	0.44	T	1893	KFLSHSTDSLNKI
Akap13	0.65		0.67	0.74	S	1892	WKFLSHSTDSLNK
Ampd2	0.55		0.68	0.72	S	63	RSGLGASPLQSAR
Arhgef1	0.39	0.67	0.64		T	432	GPTRRATPEPGDD
Cfl1	0.49		0.45	0.49	S	3	____MASGVAVSD
Clcc1	0.37		0.36	0.52	S	434	LRQRFHSGNKSPE
Coro1a	0.43	0.34	0.55	0.77	T	418	SARRRATPEPSGT
Dstn	0.62	0.69	0.64	0.46	S	3	____MASGVQVAD
Evl		0.44	0.45	0.46	S	353	TPSVAKSPEAKSP
Fyb	0.44	0.49	0.56	0.67	S	561	VEIDYDSLKRKKN
Hmha1	0.66	0.45	0.47	0.45	S	23	KKNRAGSPNPQSS
Larp1		0.42	0.45	0.69	T	770	GSPRAVTPVPTKT
Larp1	0.45	0.43	0.51	0.92	S	1010	PSTIARSLPTTVP
Nfatc2	0.29	0.44	0.33	0.32	S	136	GRDAGLSPEQPAL
Osbpl11	0.48		0.54	0.68	S	192	LASSGNSPISQRR
Plekho2	1.24	0.28	0.40	0.30	S	395	FHPRSSSLGDLLR
Prkd2	0.20		0.70	0.47	S	211	HSVRLGSSESLPC
Rasal3	0.51		0.28	0.49	S	887	WTRASASLPRKPS
Rasal3	0.67		0.71	0.61	S	818	KSQSLRSFQGAGS
Rbl1	0.65	0.70	0.61	0.89	S	1036	ISGDADSPAKRLC
Tbc1d15	0.71	0.33	0.27	0.39	S	205	NKSLSQSFENLLD
Tmpo	0.59		0.32	0.71	S	157	QGTESRSSTPLPT

Table 4

List of kinases predicted to be active and number of sites found consistently (found in at least 3 out of 4 experiments) phosphorylated in CTL using MaxQuant software analysis. MaxQuant uses a sequence window ± 6 amino acids around the identified phosphorylation site to determine the kinase that could phosphorylate this motif.

Kinase	Sites
AURORA	8
AURORA-A	19
CAMK2	56
CDK1	21
CDK2	40
CHK1	3
CHK1/2	27
CK1	53
CK2	63
ERK/MAPK	23
GSK3	11
NEK6	16
NIMA	7
PIM1/2	6
PKA	101
PKA/AKT	67
PKC	3
PKD	14
PLK	3
PLK1	3
Unspecified	198
	742

Europe PMC Funders Author Manuscripts

Nat Immunol. Author manuscript; available in PMC 2011 October 01.

Table 5

Phosphorylated chromatin regulators in CTLs. List of selected proteins from the Ingenuity Pathway Analysis transcription group of consistent (found in at least 3 out of 4 experiments) phosphorylations with known chromatin regulation function with the ratio (TCR stimulated/unstimulated) and phosphorylation sites/sequences

	Ratio (TCR stimulated/unstimulated)						
Gene Name	**Exp1**	**Exp2**	**Exp3**	**Exp4**	**Aa**	**Position**	**Sequence.Window**
Aebp2		1.03	0.77	0.94	S	24	SPLSPGSPGPAAR
Aebp2		1.77	1.23	0.93	S	21	SRLSPLSPGSPGP
Cbx3	0.90	1.02	1.14		S	95	TKRKSLSDSESDD
Cbx3	1.42	1.15	1.22		S	93	DGTKRKSLSDSES
Cbx5	2.31		2.01	2.44	S	93	GNKRKSSFSNSAD
Dnmt1		0.60	0.39	2.69	S	32	TLSVETSPSSVAT
Hdac1	1.11		0.93	1.08	S	421	ACEEEFSDSDEEG
Hdac1	1.11		0.93	1.08	S	423	EEEFSDSDEEGEG
Hdac2	1.28		0.81	0.98	S	422	ACDEEFSDSEDEG
Hdac2	1.28		0.81	0.98	S	424	DEEFSDSEDEGEG
Hdac7	0.87		0.85	1.01	S	204	PLLRKESAPPSLR
Hdac7	1.07		1.04	0.97	T	342	HRPLNRTRSEPLP
Hdac7	0.89		1.13	0.99	S	178	PLRKTVSEPNLKL
Helb	0.89	0.85	0.84	0.96	S	1015	FPFDEESPSKFRM
Helb	0.92	0.92	0.94	0.96	S	1017	FDEESPSKFRMVE
Helb	1.26	1.22	1.30		S	946	FASQPSSPRVGGR
Hsf1	1.35	1.03	1.00		S	303	VKQEPPSPPHSPR
Hsf1	1.35	1.03	1.00		S	307	PPSPPHSPRVLEA
Kdm5c		1.18	1.31	0.90	S	897	LVSQPSSPGLLQS
Lrch4		2.62	0.90	1.17	S	25	SVSLPGSPGLPGS
Ncor1	1.06	2.17	1.65	0.94	S	1482	APKAQLSPGLYDD
Ncor2	1.31	1.06	1.00		S	152	EPVSPPSPPHADP
Ncor2	1.47	1.06	1.00		S	149	GKLEPVSPPSPPH
Ptma	0.92	1.00	1.07		S	54	PACPTMSDAAVDT

	Ratio (TCR stimulated/unstimulated)						
Gene Name	**Exp1**	**Exp2**	**Exp3**	**Exp4**	**Aa**	**Position**	**Sequence.Window**
Rnf20	0.94	0.99	0.83		S	138	PEPDSDSNQERKD
Smarcc2		0.96	1.04	1.04	S	283	LTDEVNSPDSDRR
Trim28	1.44	1.46	0.97	1.15	S	23	ASAASGSPGSGEG
Trim28	4.82	4.77	3.79		S	471	VSGMKRSRSGEGE
Trim28	4.49	4.81	3.71	1.94	S	473	GMKRSRSGEGEVS

Europe PMC Funders Author Manuscripts

Europe PMC Funders Author Manuscripts

Table 6

Phosphorylated chromatin regulators in CTLs: class II histone deacetylase 7 (HDAC7). HDAC7 phosphorylation sites found in four independent SILAC experiments after HILIC/IMAC and 14-3-3 affinity purification.

TCR stim./ no stim.						
Exp 1	**Exp 2**	**Exp 3**	**Exp 4**	**Aa**	**Position**	**Sequence Window**
0.87		0.85	1.01	S	204	PLLRKEpSAPPSLR
1.07		1.04	0.97	T	342	HRPLNRpTRSEPLP
0.89		1.13	0.99	S	178	PLRKTVpSEPNLKL
	0.99	0.86	1.01	14-3-3 affinity purification		

Europe PMC Funders Author Manuscripts

Table 7

Fold change of GFP-HDAC7-ΔP expressing cells relative to control (GFP negative cells) of selected genes with cytokine receptor function found in the microarray analysis. *ns= non-significant change.

Gene Symbol	Gene name	Fold change
Il2ra	interleukin 2 receptor, alpha chain;CD25	0.19
Ccl5	chemokine (C-C motif) ligand 5; RANTES	0.52
Ccl4	chemokine (C-C motif) ligand 4; MIP-1B	0.52
Cd27	CD27 antigen; Tnfrsf7	1.45
Il6st	interleukin 6 signal transducer; CD130	1.86
Il2rg	interleukin 2 receptor, gamma chain; CD132	1.94
Il2rb	interleukin 2 receptor, beta chain; CD122	ns
Il4ra	interleukin 4 receptor, alpha; CD124	ns
Il6ra	interleukin 6 receptor, alpha; CD126	ns
Il7r	interleukin 7 receptor; CD127	ns
Il12rb1	interleukin 12 receptor, beta 1; CD212	ns
Il12rb2	interleukin 12 receptor, beta 2	ns
Il15ra	interleukin 15 receptor, alpha chain	ns
Ifngr1	interferon gamma receptor 1; CD119	ns
Ifngr2	interferon gamma receptor 2	ns

Europe PMC Funders Author Manuscripts

Table 8

Fold change of GFP-HDAC7-ΔP expressing cells relative to control (GFP negative cells) of selected genes with anti- and pro-apoptotic activity found in the microarray analysis. *ns= non-significant change.

	Gene Symbol	Gene name	Fold change
Anti-apoptotic	Bcl2	B-cell leukemia/lymphoma 2	1.54
	Mcl1	myeloid cell leukemia sequence 1	2.01
	Bcl2l1 (Bcl2-x)	BCL2-like 1	ns
	Bcl2l2 (Bcl-w)	BCL2-like 2	ns
	Bcl2l10 (Bcl-b)	Bcl2-like 10	ns
	Bcl2a1a (Bcl2a1)	B-cell leukemia/lymphoma 2 related protein A1a	ns
Pro-apoptotic	Bcl2l11 (Bim)	BCL2-like 11 (apoptosis facilitator)	ns
	Bbc3 (Puma)	BCL2 binding component 3	ns
	Pmaip1 (Noxa)	phorbol-12-myristate-13-acetate-induced protein 1	0.42
	Bid	BH3 interacting domain death agonist	ns
	Bax	BCL2-associated X protein	0.58
	Fas	Fas (TNF receptor superfamily member 6)	ns
	Fasl	Fas ligand (TNF superfamily, member 6)	0.36
	Trp53	p53	ns
	Apaf1	apoptotic peptidase activating factor 1	1.24
	Cradd	CASP2 and RIPK1 domain containing adaptor with death domain; RAIDD	0.43
	Nr4a1 (Nur77)	nuclear receptor subfamily 4, group A, member 1	0.43